

Supporting information for:
Charge carrier loss mechanisms in $\text{CuInS}_2/\text{ZnO}$
nanocrystal solar cells

Dorothea Scheunemann,* Sebastian Wilken, Jürgen Parisi, and Holger Borchert

*Energy and Semiconductor Research Laboratory, Department of Physics, University of
Oldenburg, Carl-von-Ossietzky-Straße 9–11, 26129 Oldenburg, Germany*

E-mail: dorothea.scheunemann@uni-oldenburg.de

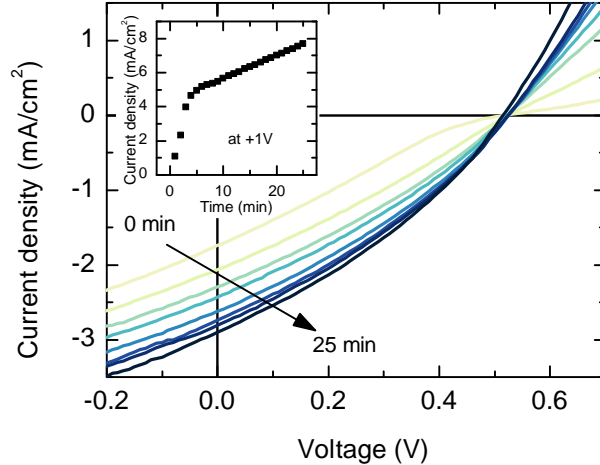


Figure S1: J - V characteristics of a representative $\text{CuInS}_2/\text{ZnO}$ solar cell as a function of the exposure time to continuous AM1.5G illumination (light soaking). After 25 min of light-soaking, an open-circuit voltage of 0.52 V, a short-circuit current density of 2.9 mA/cm^2 , a fill factor of 33 %, and a power conversion efficiency of 0.5 % is obtained, respectively. Inset: Time development of the current density at a forward bias voltage of 1 V.

Charge transport properties of pure NC ZnO films To study the charge transport in pure NC ZnO films, we used an approach described in detail in Ref. 1. Briefly, ZnO NC films with a thickness of $d \approx 50$ nm were spin-coated on glass and annealed at 180 °C for 10 min in an inert atmosphere (N_2 -filled glovebox; same conditions as for solar cell preparation). Subsequently, two Al electrodes with a thickness of 120 nm and a lateral spacing of $L \approx 80$ μm were thermally evaporated under high vacuum (1×10^{-6} mbar) on top of the ZnO. In that specific device configuration, the conducting channel between the Al electrodes is in direct contact to the ambient gas. Current-voltage (I - V) characteristics of the devices were recorded in the dark and under UV illumination ($\lambda = 350$ nm, $1 \text{ mW}/\text{cm}^2$) with a source-measuring unit (Keithley 2400). Measurements were subsequently performed under inert and ambient conditions.

Under inert conditions (Figure S2a), a linear scaling of the I - V curve can be observed both in the dark and under UV illumination, indicating ohmic conduction over the whole range of applied bias voltages ($I \propto V$). Notably, the current, and thereby the conductivity, increased by several orders of magnitude upon UV illumination (photoconduction). In

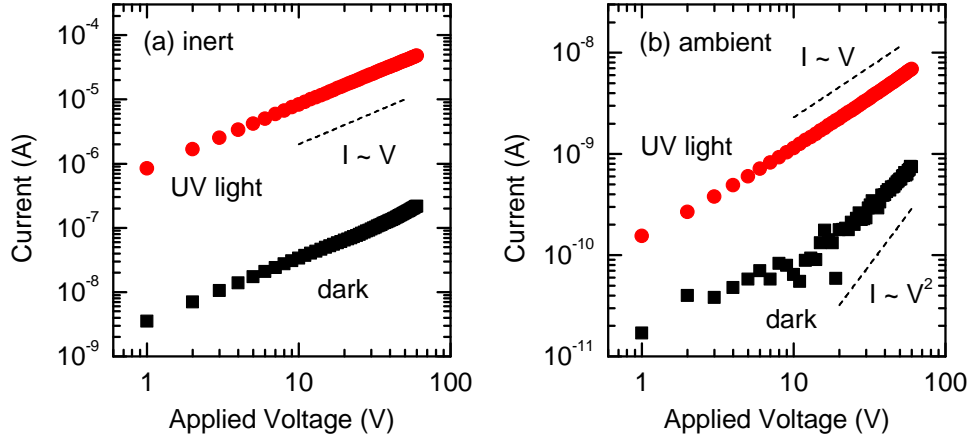


Figure S2: I - V characteristics of ZnO thin films on glass with laterally spaced Al electrodes, recorded (a) under nitrogen atmosphere and (b) in ambient air. Measurements were performed in the dark (filled symbols) and under exposure with UV light ($\lambda = 350$ nm, 1 mW/cm², open symbols). Dashed lines show the scaling expected for ohmic ($I \propto V$) and space-charge limited conduction ($I \propto V^2$).

contrast, when exposed to ambient air (Figure S2b), the dark I - V characteristics exhibit a transition to higher scaling exponents (super-linear behavior) at high voltage, with the slope approaching the limit for trap-free space-charge limited conduction ($I \propto V^2$). In contrast, in the presence of UV light, the I - V characteristics shift to ohmic conduction again.

From the the linear region of the I - V characteristics ($V \leq 10$ V), we estimated the specific conductivity σ of the ZnO films according to

$$\sigma = \frac{I}{V} \frac{L}{d \cdot w}, \quad (1)$$

where L is the spacing between the electrodes, w the electrode width, and d the thickness of the ZnO film. Table S1 lists the resulting values of σ under the different experimental conditions. It can be seen that under exposure to ambient air, the dark conductivity decreased by 3 orders of magnitude and the photoconductivity by 4 orders of magnitude compared to inert conditions. We attribute this finding to the depletion of mobile carriers due to the surface adsorption of oxygen species, as described in detail previously.¹

Table S1: Conductivity of ZnO films under different experimental conditions.

Atmosphere	Illumination	Conductivity σ (S/m)
inert ^a	dark	1.4×10^{-3}
	UV light	3.3×10^{-1}
ambient	dark	5.6×10^{-6}
	UV light	4.4×10^{-5}

^a N₂ atmosphere with a residual oxygen content of less than 3 ppm.

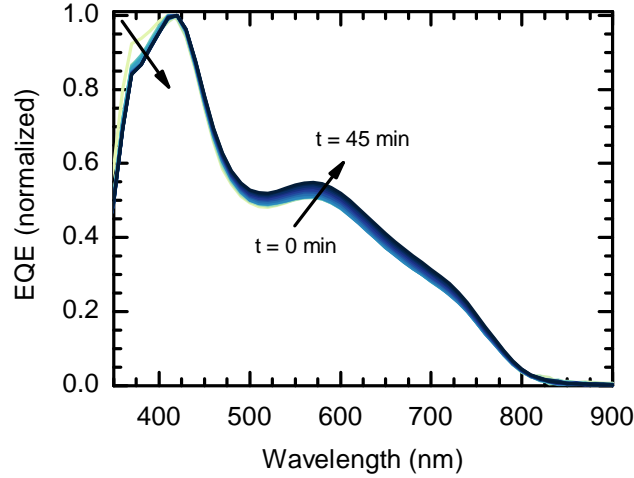


Figure S3: EQE spectra normalized at $\lambda = 420$ nm for a representative device as a function of the UV exposure time (0 to 45 min). Here, $t = 0$ min is defined as the state where the EQE signal was completely relaxed to a stable state. Only small variation of the spectral shape can be seen with increasing illumination time.

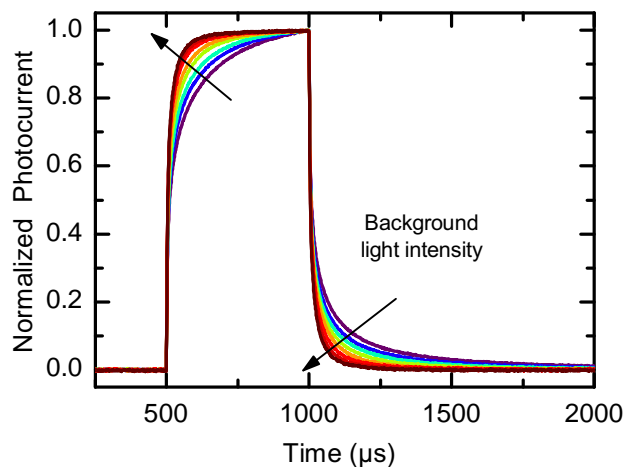


Figure S4: Normalized photocurrent transients as a function of the white-light background illumination intensity (dark to ~ 0.7 suns; zero bias voltage).

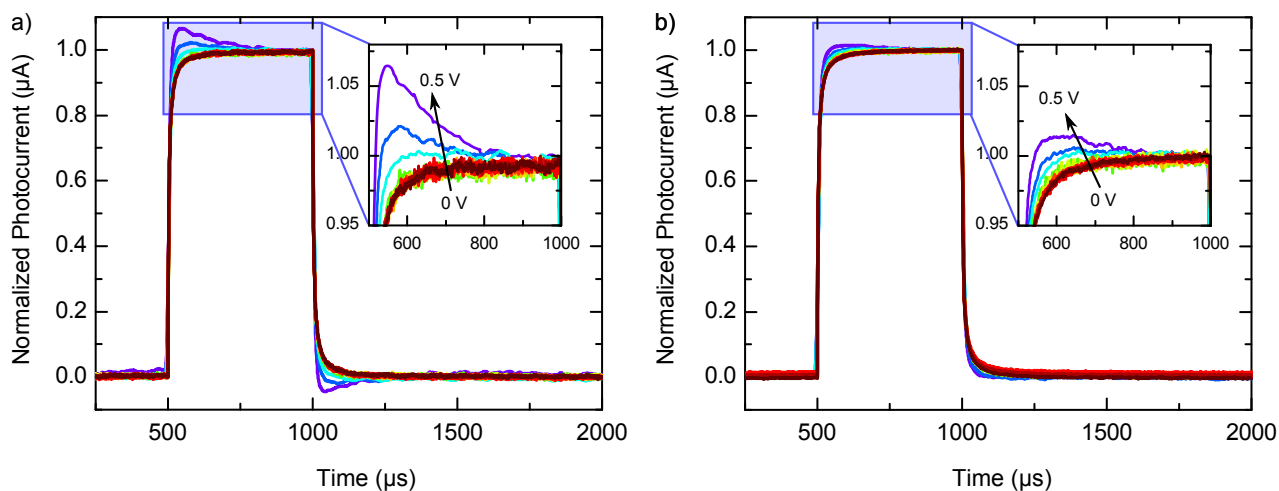


Figure S5: Normalized TPC signals at variable bias voltage (0 to 0.5 V) under (a) solely WL and (b) WL + UV background illumination. Without UV light present (panel a), a pronounced overshoot behavior (i.e., the current exceeds its steady-state value right after switching on/off the pulse excitation) can be seen at applied voltages near V_{oc} . In the presence of UV light (panel b), the overshoots are clearly reduced.

TPV Measurements To determine the small-perturbation carrier lifetime, we tried to fit the transient photovoltage signal both to a monoexponential decay function, $\Delta V(t) = A_1 \exp(-t/\tau_1)$, and a biexponential decay function, $\Delta V(t) = A_1 \exp(-t/\tau_1) + A_2 \exp(-t/\tau_2)$, where A_1, A_2 and τ_1, τ_2 are scaling and time constants, respectively. Figure S6 shows that only the biexponential model is able to describe the data well, as indicated by the random distribution of the residuals around zero. In contrast, the monoexponential model gives a poor fit of the data with clearly patterned residuals. During the experiments, the light pulse was attenuated such that $\Delta V < 1$ mV for all background illumination intensities applied. Hence, the excess carrier concentration due to the perturbation is assumed sufficiently small compared to the steady-state concentration (low-level injection), so that the recombination rate can be linearized over the whole range of open-circuit voltages. Therefore, we propose that the occurrence of two carrier lifetimes τ_1, τ_2 is related to two different recombination channels, rather than a transition from the high- to the low-level injection regime.

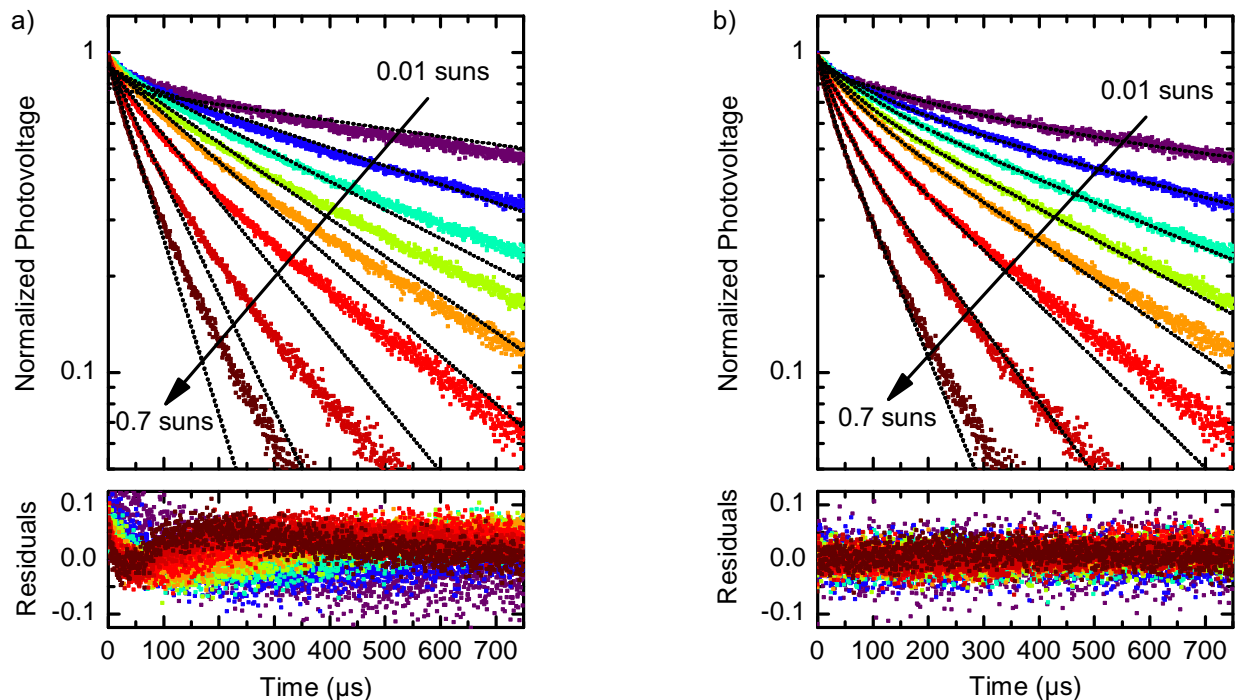


Figure S6: Fitting of the TPV data to (a) monoexponential and (b) biexponential decay functions. Photovoltage transient were recorded under variable WL background illumination intensity (~ 0.01 to 0.7 suns). The bottom panels show the corresponding residuals.

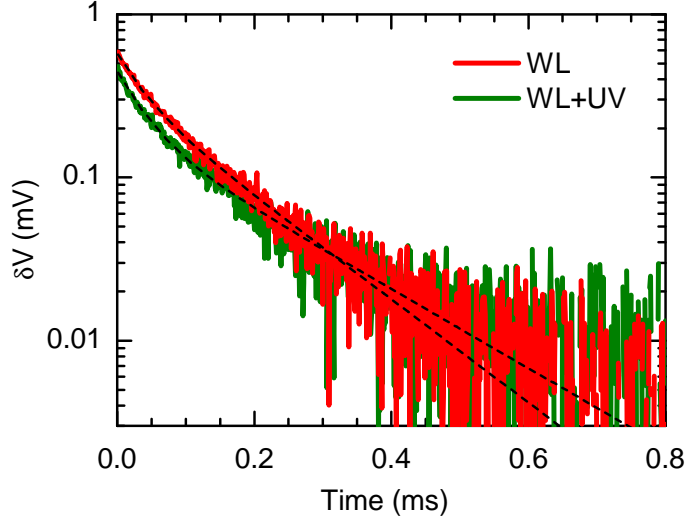


Figure S7: Voltage decay for TPV measurements under solely WL and WL + UV background illumination, respectively. In both cases, the WL intensity was about 0.7 suns. Dashed lines indicate fits of the experimental data to a biexponential decay function.

Recently, Chang et al.² reported similar results for nanostructured PbS/ZnO solar cells and attributed the two recombination channels to bulk and interface recombination, respectively. This hypothesis is based on the comparison of TPV experiments on devices without and with a surface passivation of the ZnO, the latter being obtained by introducing an additional TiO₂ interlayer. With the passivation, the authors observed that the relative importance of the faster decay channel (attributed to interfacial recombination) significantly decreased, while the time constant of the slower decay channel (attributed to bulk recombination) increased by one order of magnitude. Both effects were explained by a reduced interfacial recombination rate due to the passivation of traps at the ZnO surface.

In the present work, we used photodoping with UV light to modulate the ZnO surface trap density, which is shown to have strong impact on the charge collection in our CuInS₂/ZnO devices (see main text). In order to test whether these effects are related to interface recombination, we conducted TPV measurements with and without an UV component added to the WL background illumination. Figure S7 shows the raw data fitted to a biexponential decay function, while Table S2 lists the resulting fit parameters. It is clearly seen that the additional UV light has no significant effect on both the time constants and the relative weights

of the respective decay channels. Hence, in clear contrast to Chang et al.,² the surface trap density apparently plays only a marginal role in the recombination behavior at open circuit. Therefore, we suppose that the two independent decay channels are related to two different recombination paths within the bulk, rather than bulk and interface recombination.

Table S2: Fit parameters obtained for TPV measurements under WL and WL + UV background illumination, respectively.

Illumination	$A_1/(A_1 + A_2)$	τ_1 (ms)	$A_2/(A_1 + A_2)$	τ_2 (ms)
only WL	0.43	0.037	0.57	0.14
WL + UV	0.56	0.040	0.44	0.18

References

- (1) Wilken, S.; Parisi, J.; Borchert, H. Role of Oxygen Adsorption in Nanocrystalline ZnO Interfacial Layers for Polymer-Fullerene Bulk Heterojunction Solar Cells. *J. Phys. Chem. C*. **2014**, *118*, 19672–19682.
- (2) Chang, J.; Kuga, Y.; Mora-Seró, I.; Toyoda, T.; Ogomi, Y.; Hayase, S.; Bisquert, J.; Shen, Q. High Reduction of Interfacial Charge Recombination in Colloidal Quantum Dot Solar Cells by Metal Oxide Surface Passivation. *Nanoscale* **2015**, *7*, 5446–5456.